**Proceedings of the ASME 2013 International Design Engineering Technical Conferences and Computers and Information in Engineering Conference**
**IDETC/CIE 2013**
**August 4-7, 2013, Portland, Oregon, USA**

**DETC2013-12138**

# THERMAL AND MECHANICAL RESPONSES OF PARTICULATE COMPOSITE PLATES UNDER DIRECT EXCITATION

**Jacob K. Miller, Jeffrey F. Rhoads***
School of Mechanical Engineering,
Ray W. Herrick Laboratories
Purdue University
West Lafayette, Indiana 47907
Email: jfrhoads@purdue.edu

## ABSTRACT

*The thermal and mechanical near-resonant responses of particulate composite plates formed from hydroxyl-terminated polybutadiene (HTPB) binder and varying volume ratios of $NH_4CL$ crystals (50, 65, 75%) are investigated. Each plate is mounted and forced with three levels of band-limited, white noise excitation (10-1000 Hz at 1.00, 1.86 and 2.44 g RMS). The mechanical response of each plate is recorded via scanning laser Doppler vibrometry. The plates are then excited at a single resonant frequency and the thermal response is recorded via infrared thermography. Comparisons are made between the mechanical mode shapes of each plate and spatial temperature distributions, with correlation seen between stress/strain and heat generation. The effects of the various crystal/binder ratios on both the thermal and mechanical responses are discussed. Results are also compared to numerical simulations. The observed thermomechanical effects help render an improved understanding of the thermomechanics of plastic-bonded composites, an essential step in support of the development of new technologies for the vapor-based detection of hidden explosives.*

## 1 INTRODUCTION

The development of new technologies designed to detect hidden explosive threats is an essential research area for both national security and defense. While a wide array of detection systems are currently in development or use, the most popular often seek to leverage trace vapor detection technologies [1,2]. Despite the potential of this approach, the trace vapor detection of composite explosives remains a significant technical challenge [2], particularly in highly-dynamic detection environments. Interestingly, the vapor pressures of many explosives materials are strongly dependent on temperature, and may be greatly increased by heating [1]. Thus, the induction of heat within such materials should prove highly beneficial in increasing the detection probabilities associated with various stand-off detection technologies.

Given that low-frequency excitations can be transmitted across comparatively large distances, the thermal response of particulate composite materials, in particular plastic-bonded explosives, to low-frequency excitations (acoustic or mechanical in nature) is of distinct interest. Unfortunately, few thorough studies of the thermomechanics of particulate composite materials to low-frequency excitations currently exist. While the works of Loginov [3,4] provide some insight in this regard, these works focus largely on the phenomenological nature of the heating, rather than its selective control or the impact of the particle/binder ratio.

In previous works, the material properties of particulate composites as a function of particle/binder ratio have been well documented. Not surprisingly, these works have revealed that the bulk thermal and mechanical modulii of such materials vary dramatically with particle/binder ratio [5–7]. For example, Lewis [8] observed an inverse relationship between particle/binder ra-

*Address all correspondence to this author.

tios and damping ratios, and noted that this may be attributable to mismatched thermal expansion coefficients.

In many pure materials and alternative composites, the mechanisms of heat generation in response to acoustic and ultrasonic excitation is a well-studied effect. For example, these studies have highlighted the fact that the heating within materials due to cyclic deformation is often attributable to a phase delay between fluctuating stress and strain fields [9]. In the context of vibrothermography, Renshaw [10] and others [11–13] have shown that high-frequency excitation is highly effective at eliciting thermal responses near stress concentrations, such as cracks, voids, and inclusions. While most of the work in this field specifically targets heating near defects, research in this area has also highlighted stress-induced heating along the modal structure of various systems [14–16]. As vibrothermography is primarily used in the nondestructive testing of damaged samples, excitation at structural resonance is generally avoided, as heating from modal deflection patterns may cause damage effects to become more difficult to identify [17].

The objectives of this work were to observe and characterize the thermal and mechanical responses of plates comprised of hydroxyl-terminated polybutadiene (HTPB) binder and ammonium chloride ($NH_4CL$) crystals under direct, low frequency (10-1000 Hz) excitation. These plates serve as mechanical mock materials of common plastic-bonded explosives. The plates were mounted directly to an electrodynamic shaker to deliver the greatest possible excitation energy. Heat generation induced via this external excitation was quantified at various resonance frequencies via infrared thermography. The dependence of heat generation on the crystal/binder ratio is discussed. As previously highlighted, it is hoped that the observed thermomechanical effects will help render an improved understanding of the thermomechanics of plastic-bonded composites, an essential step in support of the development of new technologies for the vapor-based detection of hidden explosives.

## 2 EXPERIMENTAL TECHNIQUE

### 2.1 SAMPLE PREPARATION

As noted above, this work focuses on the thermomechanics of a mock plastic-bonded explosive material comprised of an HTPB binder and $NH_4CL$ crystals. HTPB is a commonly employed binder material and the $NH_4CL$ crystals were chosen in order to approximate the particle sizes of ammonium perchlorate (AP). The volume ratio of crystal to binder may vary significantly in real world explosives, and the effect of such changes on the mechanical and thermal responses of the bulk material is of importance to this paper.

To create the samples, the HTPB was heated to 60° C and an isocyanate hardening agent was applied. A wetting agent, Tepanol, was employed before insertion and mixing of the $NH_4CL$ crystals. For samples of high volume ratio, a Resodyn acoustic mixer was employed to ensure a homogeneous mixture. The crystal/binder mixture was then poured into a purpose-built plate mold, and each was cured overnight into plates measuring 24.4 x 17.78 cm (10 x 7 in.). For the purposes of this paper, three plates were used: 50, 65 and 75% volume ratio of crystal to binder. The mass and density of each plate is presented in Table 1. As noted in the Table, the 75% plate is significantly less dense than either of the other plates. As the density of the crystal is significantly greater than that of the binder, this effect was not expected and is likely due to voids in the material. Difficulties in packing the more dense mixture into the mold were also noted.

**TABLE 1**: PLATE MATERIAL PROPERTIES.

| Volume Fraction | Mass (kg) | Density (kg/m$^3$) |
|---|---|---|
| 50% | 0.6656±0.0005 | 1154±10 |
| 65% | 0.8189±0.0005 | 1297±17 |
| 75% | 0.6460±0.0005 | 1086±15 |

### 2.2 EXPERIMENTAL SETUP

To provide mechanical excitation to the plates, a TIRA 59335/LS AIT-440 electrodynamic shaker was employed, allowing for band-limited white noise excitation. The system was controlled by a VibeLab VL-144 vibration control system through direct monitoring of a shaker head mounted accelerometer. A custom plate fixture was machined to simulate clamped boundaries on the opposite short ends of the plates, approximating clamped-free-clamped-free (CFCF) boundary conditions. The final setup yielded a 22.86 x 17.78 cm (9 x 7 in.) unsupported area. To record the frequency responses and operational deflection shapes (ODS) of each plate, a Polytec PSV-400 scanning laser Doppler vibrometer was employed. The instantaneous shaker acceleration was recorded via an accelerometer on the shaker head. To allow for improved measurements and to avoid laser diffusion through the slightly translucent plate samples, an opaque spray was applied to the plate surfaces.

For the purposes of the mechanical response, broadband (10-1000 Hz) white noise was applied at three distinct forcing levels (1, 1.86 and 2.44 g RMS). Operational deflection shapes were recorded at the highest level of forcing and were not seen to qualitatively change with excitation level. The system response (characterized in terms of relative plate acceleration) was estimated through the application of the classical H1 estimator, a comparison of the measured cross-spectral density between the accelerometer and differentiated vibrometer readings to the measured power spectral density of the accelerometer. H1 frequency response estimators were calculated at all forcing levels at two distinct points; the geometric center and an 'offset' point. The latter point was offset from the center by 6.24 and 4.82 cm as

measured from the free and clamped edges, respectively. Geometrically, the offset traverses 54.6% and 54.2% of the distances between the center point and the free and clamped edges.

To capture the thermal responses of the plates, a FLIR A320 thermal camera was used to record both transient and steady-state thermal responses of the surfaces of each plate. This camera had a temperature sensitivity of 0.07° C at 30° C and accuracy of ±2° C or ±2%. The infrared data was calibrated to the emissivity of each plate through comparison to a thermocouple at ambient conditions and after the application of a heat gun. For this testing, the plates were excited at resonance for 10 minutes or until thermal steady state was reached. For the purposes of this paper, steady state implies a temperature change of less than 0.5° C over 100 seconds. The level of forcing used for thermal analysis was 6 g. In addition to the steady-state thermal responses, the transient thermal response of each plate at the first resonance was recorded at 30 second intervals until steady state was reached. No attempt was made to control either the ambient temperature or flow conditions, but both were not seen to change significantly over the course of the experiment. A picture of the entire experimental setup, in the thermal measurement configuration, is presented in Figure 1.

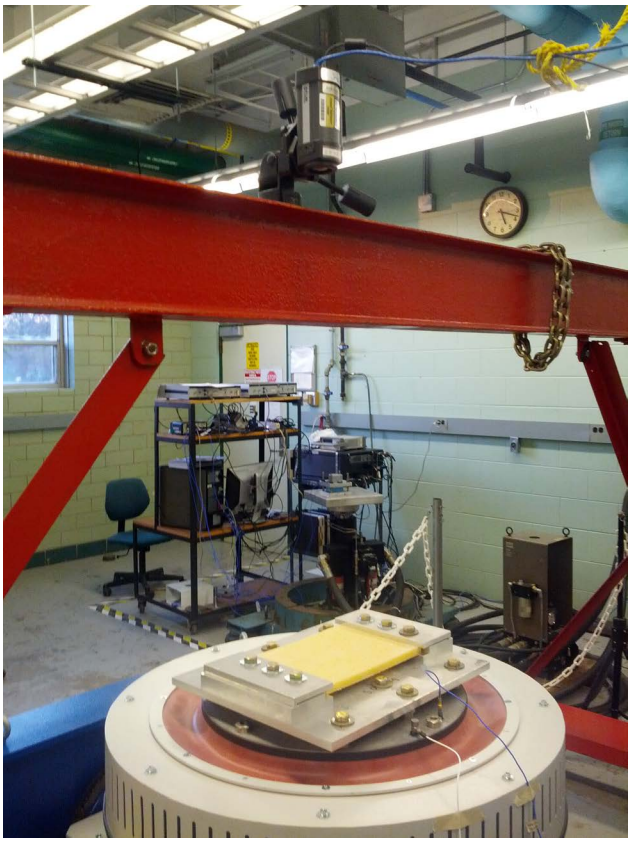

**FIGURE 1**: EXPERIMENTAL SETUP, WITH FLIR A320 INFRARED CAMERA POSITIONED ABOVE A 50% CRYSTAL VOLUME RATIO PLATE MOUNTED TO THE TIRA SHAKER BY THE CFCF CLAMPING MOUNT.

## 3 NUMERICAL SIMULATION

To obtain a point of comparison for the experimentally-recorded mechanical responses, a rudimentary ANSYS simulation of a CFCF plate of the appropriate dimensions was performed. The simulation emulated a 50% crystal volume ratio plate, using the density value reported in Table 1. The modulus of elasticity of the plate was estimated from the resonant frequency of a 50% cylindrical sample as 19.1 MPa [18]. The Poisson's ratio was estimated as 0.39, based on perceived material similarities to more common materials. The simulation utilized band-limited white noise excitation and was used to recover resonant frequencies and corresponding mode shapes.

## 4 RESULTS

### 4.1 MECHANICAL RESPONSE

The vibrometer-recorded H1 frequency response estimators of relative acceleration for each plate in response to three levels of excitation are presented as Figures 2, 3, and 4 for the 50, 65, and 75% plates, respectively. These plots present data at both the center and offset points, and provide some insight into the nature of each plate. Note that all of the plates exhibit clear resonant behavior, with multiple sharp peaks observable over the excited frequency range. The 65 and 75% plates show a slightly softening response, with peaks decreasing slightly in both amplitude and frequency as the forcing increases. These two plates also exhibit a split "first" mode, with the 75% case being more severe. Qualitatively, the higher volume fraction plates appear to have more highly-damped responses and much smoother response curves. The experimentally-obtained natural frequencies of each plate are presented in Table 2. Each frequency is nondimensionalized by its first natural frequency to allow for comparison between cases. As evident in the table, there is generally very good agreement between the nondimensionalized natural frequencies of the observed modes. The mode numbers referenced in the Table are representative of the frequency-sorted pure modes of the finite element model and do not suggest the exclusion of any data. Table 3 presents the half-power estimated bandwidth and quality factors of the first and eighth modes for each plate. The data points presented are the only ones for which the half-power method was applicable, with the other half-power levels obscured due to relatively low peak magnitudes or overlapping effects from adjacent peaks. The quality factor appears to decrease from the 50% to 75% plates, suggesting greater damping in the highest crystal case. The 65% plate shows the highest quality factor of all of the plates at the first resonance, although the difference between this and the 50% case is quite small. The

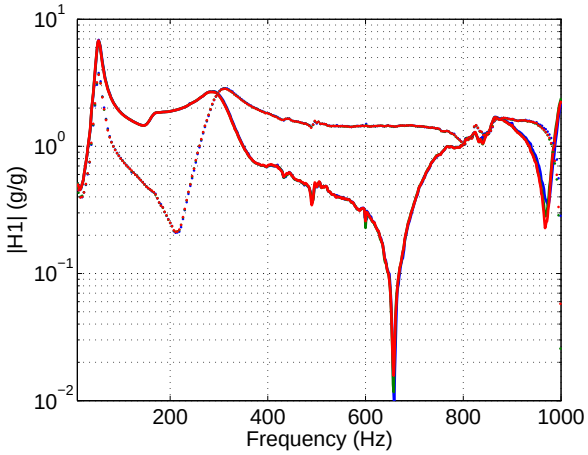


**FIGURE 2**: H1 FREQUENCY RESPONSE ESTIMATORS OF THE RELATIVE ACCELERATION OF THE 50% PLATE FOR THREE LEVELS OF EXCITATION. THE RED, BLUE AND GREEN CURVES DEPICT RESPONSES AT 2.44, 1.86, AND 1 g RMS, RESPECTIVELY. SOLID LINES REPRESENT DATA FROM THE GEOMETRIC CENTER, DASHED LINES REPRESENT DATA FROM THE OFFSET POINT. NOTE THE MULTIPLE CLEAR RESONANT FREQUENCIES, AND SMALL DIFFERENCES BETWEEN FORCE CURVES.

recorded operational deflection shapes for all cases are presented as groups of perceived matches in Figures 5-8.

### 4.2 THERMAL RESPONSE

The transient surface temperature responses of each plate at the first resonance, presented separately as the average and maximum surface temperatures of the plate, are presented in Figure 9. As visible in the figure, all of the plates asymptotically approach maximum temperature values within a 14 minute window. Notably, the 50% plate exhibits a comparatively large thermal response, nearly double that of the other plates. The 65% and 75% plates have comparable mean temperatures, but the 75% plate has a distinctly high peak value. Comparisons of the spatial surface temperature profiles and the spatial velocity profiles at first resonance are presented for each plate in Figures 10-12. Figure 13 presents the same data for the second portion of the split peak in the 75% plate case. The state of stress within the material is not calculated here due to the relatively unknown nature of the mechanical properties, but is assumed to vary with spatial derivatives, as in isotropic materials. As evident in the plots, temperature profiles are maximized at areas of presumed high stress/strain. This effect is most obvious in the changing center of heating visible in the 75% plate responses. The extraneous hot spot exhibited by the 75% plate in Figure 12 was identified as the location of a crack in the plate surface. As previously outlined,

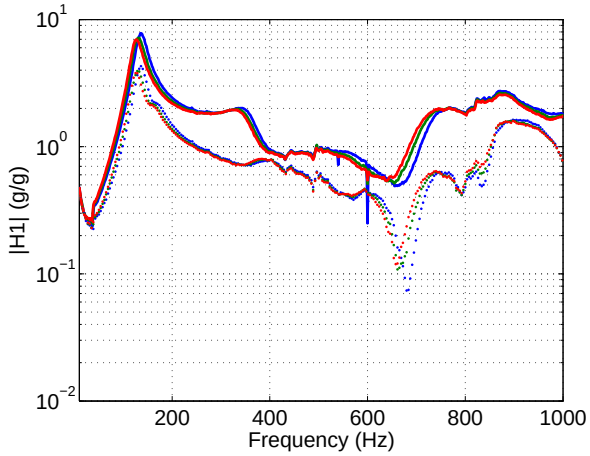


**FIGURE 3**: H1 FREQUENCY RESPONSE ESTIMATORS OF THE RELATIVE ACCELERATION OF THE 65% PLATE FOR THREE LEVELS OF EXCITATION. THE RED, BLUE AND GREEN CURVES DEPICT RESPONSES AT 2.44, 1.86, AND 1 g RMS, RESPECTIVELY. SOLID LINES REPRESENT DATA FROM THE GEOMETRIC CENTER, DASHED LINES REPRESENT DATA FROM THE OFFSET POINT. NOTE THE SLIGHTLY SPLIT FIRST PEAK, AND SLIGHTLY SOFTENING NATURE OF RESPONSES.

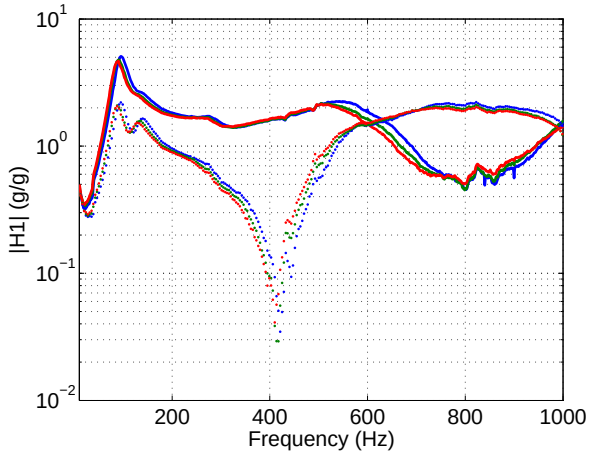


**FIGURE 4**: H1 FREQUENCY RESPONSE ESTIMATORS OF THE RELATIVE ACCELERATION OF THE 75% PLATE FOR THREE LEVELS OF EXCITATION. THE RED, BLUE AND GREEN CURVES DEPICT RESPONSES AT 2.44, 1.86, AND 1 g RMS, RESPECTIVELY. SOLID LINES REPRESENT DATA FROM THE GEOMETRIC CENTER, DASHED LINES REPRESENT DATA FROM THE OFFSET POINT. NOTE THE SPLIT FIRST PEAK, SLIGHTLY SOFTENING NATURE OF RESPONSES, AND COMPARATIVELY HIGH DAMPING.

**TABLE 2**: RESONANT FREQUENCIES FOR ALL OF THE OBSERVED OPERATIONAL DEFLECTION SHAPES.

| Plate | $f_1$ (Hz) | $f_{1B}$ (Hz) | $f_3$ (Hz) | $f_3/f_1$ | $f_8$ (Hz) | $f_8/f_1$ | $f_{22}$ (Hz) | $f_{22}/f_1$ |
|---|---|---|---|---|---|---|---|---|
| Finite Element | 33.3 | - | 83.7 | 2.52 | 169.2 | 5.09 | 385.1 | 11.58 |
| 50% | 52.5 | - | 151.3 | 2.88 | 295.0 | 5.62 | 731.3 | 13.93 |
| 65% | 126.3 | 157.5 | 351.3 | 2.78 | - | - | - | - |
| 75% | 82.5 | 126.3 | - | - | 547.5 | 6.64 | - | - |

**TABLE 3**: EXPERIMENTALLY-RECOVERED HALF-POWER BANDWIDTHS AND QUALITY FACTORS.

| Plate | $f_1$ (Hz) | Bandwidth (Hz) | Q | $f_8$ (Hz) | Bandwidth (Hz) | Q |
|---|---|---|---|---|---|---|
| 50% | 52.5 | 12.5 | 4.20 | 295.0 | 116.2 | 2.54 |
| 65% | 126.3 | 26.2 | 4.82 | - | - | - |
| 75% | 82.5 | 28.75 | 3.13 | 547.5 | 248.8 | 2.09 |

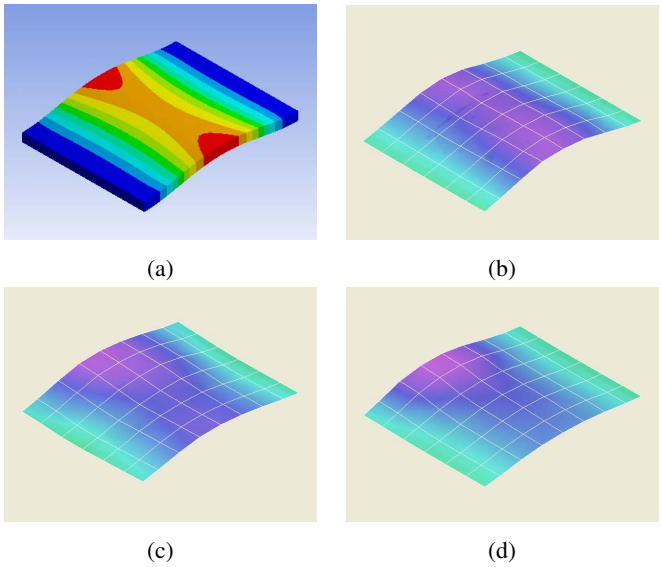


**FIGURE 5**: COMPARISON OF THE NUMERICALLY-OBTAINED MODE SHAPES AND EXPERIMENTALLY-OBTAINED OPERATIONAL DEFLECTION SHAPES, NEAR THE 1ST RESONANT FREQUENCY. (a) MODE SHAPE OF A 50% PLATE AT 33.3 HZ. (b) ODS OF A 50% PLATE AT 52.5 HZ. (c) ODS OF A 65% PLATE AT 126.3 HZ. (d) ODS OF A 75% PLATE AT 82.5 HZ.

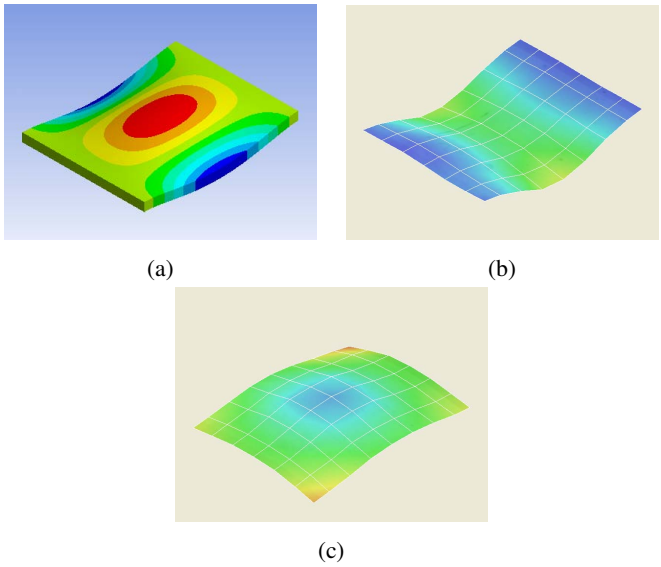


**FIGURE 6**: COMPARISON OF THE NUMERICALLY-OBTAINED MODE SHAPES AND EXPERIMENTALLY-OBTAINED OPERATIONAL DEFLECTION SHAPES, NEAR THE 3RD RESONANT FREQUENCY. (a) MODE SHAPE OF A 50% PLATE AT 83.7 HZ. (b) ODS OF A 50% PLATE AT 151.3 HZ. (c) ODS OF A 65% PLATE AT 351.3 HZ.

stress concentrations, such as this defect, are often the target of heating in vibrothermography applications. As the temperature level recorded in the defect is at the same level as the modal pattern, the effect of this defect on Figure 9b is considered to be minimal. The effect on Figure 9a is unknown. Interestingly, thermal analysis of higher frequency modes exhibited some evidence of parity with expected stress levels, but the extremely low levels of heating recorded do not allow for acceptable inclusion at this time.

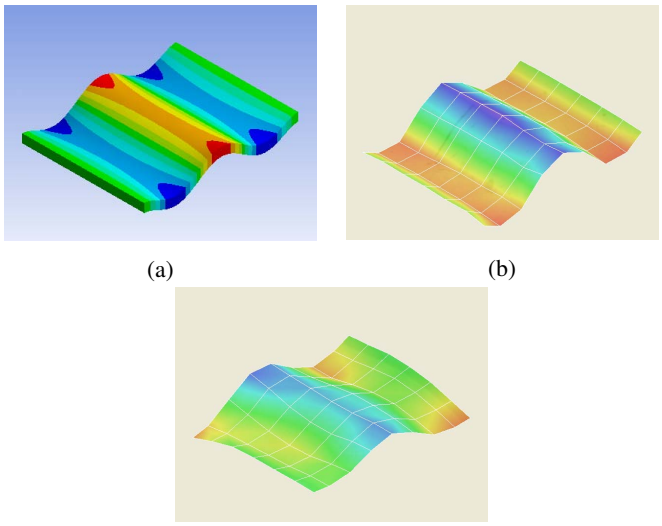

(a) (b)

(c)

**FIGURE 7**: COMPARISON OF THE NUMERICALLY-OBTAINED MODE SHAPES AND EXPERIMENTALLY-OBTAINED OPERATIONAL DEFLECTION SHAPES, NEAR THE 8TH RESONANT FREQUENCY. (a) MODE SHAPE OF A 50% PLATE AT 169.2 HZ. (b) ODS OF A 50% PLATE AT 295.0 HZ. (c) ODS OF A 75% PLATE AT 547.5 HZ.

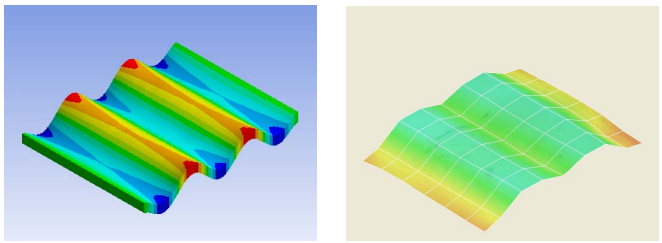

(a) (b)

**FIGURE 8**: COMPARISON OF THE NUMERICALLY-OBTAINED MODE SHAPES AND EXPERIMENTALLY-OBTAINED OPERATIONAL DEFLECTION SHAPES, NEAR THE 22ND RESONANT FREQUENCY. (a) MODE SHAPE OF A 50% PLATE AT 385.1 HZ. (b) ODS OF A 50% PLATE AT 731.3 HZ.

## 5 DISCUSSION AND CONCLUSIONS

The thermal and mechanical responses of particulate composite plates, composed of various ratios of $NH_4CL$ crystals and HTPB binder, under direct excitation has been presented. Each plate was shown to exhibit clear resonant behavior, with several distinct modal structures. The results presented herein reveal near-resonant behaviors which are strongly dependent on the particle/binder volume fraction associated with the sample. For example, an increase in the volume of crystals relative to binder appears to increase the effective bulk damping level within the material. This effect is likely due to internal friction effects attributable to particle-particle interactions at the micro-scale.

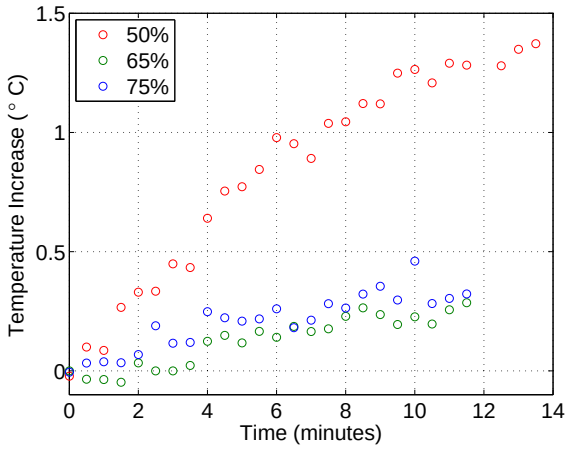


(a)

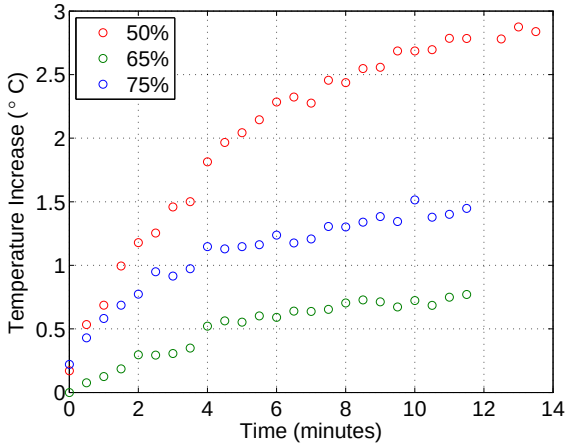


(b)

**FIGURE 9**: COMPARISON OF THE EXPERIMENTALLY-OBTAINED PLATE SURFACE TEMPERATURES VS. TIME IN RESPONSE TO A 6 g EXCITATION NEAR THE 1ST RESONANT FREQUENCY. DATA IS PRESENTED FOR (a) MEAN AND (b) MAXIMUM PLATE SURFACE TEMPERATURE VS. TIME

The steady-state surface temperature profiles reported here appear to exhibit modal structure similar to those of the velocity profile within the plates and in agreement with an isotropically-predicted stress field. In general, the thermal response of the materials echoes the state of stress in the material. This conclusion is supported by the defective 75% plate, which shows high levels of thermal response around a surface crack. As illustrated

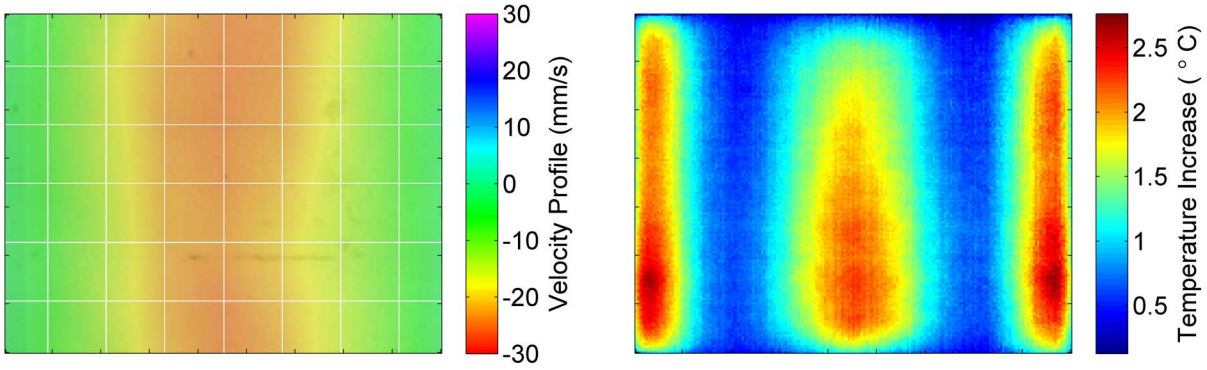


**FIGURE 10**: COMPARISON OF THE OBSERVED VELOCITY PROFILE AND THE STEADY-STATE SURFACE TEMPERATURE DISTRIBUTION OF THE 50% PLATE NEAR THE FIRST RESONANCE.

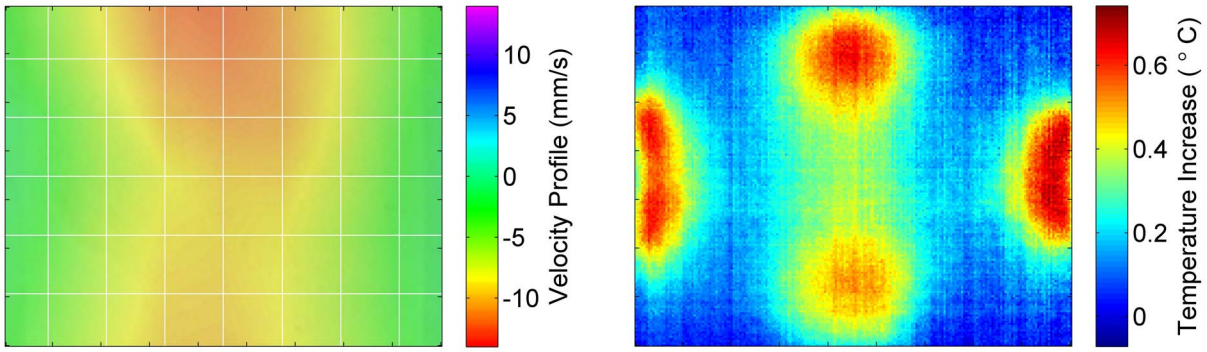


**FIGURE 11**: COMPARISON OF THE OBSERVED VELOCITY PROFILE AND THE STEADY-STATE SURFACE TEMPERATURE DISTRIBUTION OF THE 65% PLATE NEAR THE FIRST RESONANCE.

by the high magnitude thermal response of the 50% plate, heating appears to be maximized for highly viscous materials. As classically predicted, thermal effects will be maximized when the phase delay between stress and strain is maximized, an effect congruent with highly viscous materials. The level of heating, however, also appears to rise with high crystal volume ratios. This effect, like that of the observed damping increase, is likely due to interactions on the particle scale, where direct particle interactions may lead to significant stress concentrations exacerbated by the resonant excitation. This effect may be exploited to elucidate high magnitude thermal responses within high particle ratio particulate composite structures. In particular, exploitation of this high crystal ratio heating may prove useful in support of current vapor trace explosives detection methods. As low frequency excitation may be used over long distances, such excitation could prove effective at stand-off heating, thus enabling the detection of relatively large, hidden explosive devices in a fieldable detection system.

The selective targeting of higher-frequency resonant peaks did not reveal significant heat generation. The complexity of the modal patterns predicts a significant increase in the forcing required to achieve the same levels of stress and, theoretically, similar thermal responses. It is thus expected that higher-frequency resonant peaks will not be as efficient for thermal energy delivery, and that hypothetical stand-off excitation systems would be best suited to target a structure's first resonance.

Future work will attempt to more completely investigate the relationship between particle/binder ratio and the thermomechanical responses of various particulate composite materials, including explosives, through theory and experimentation.

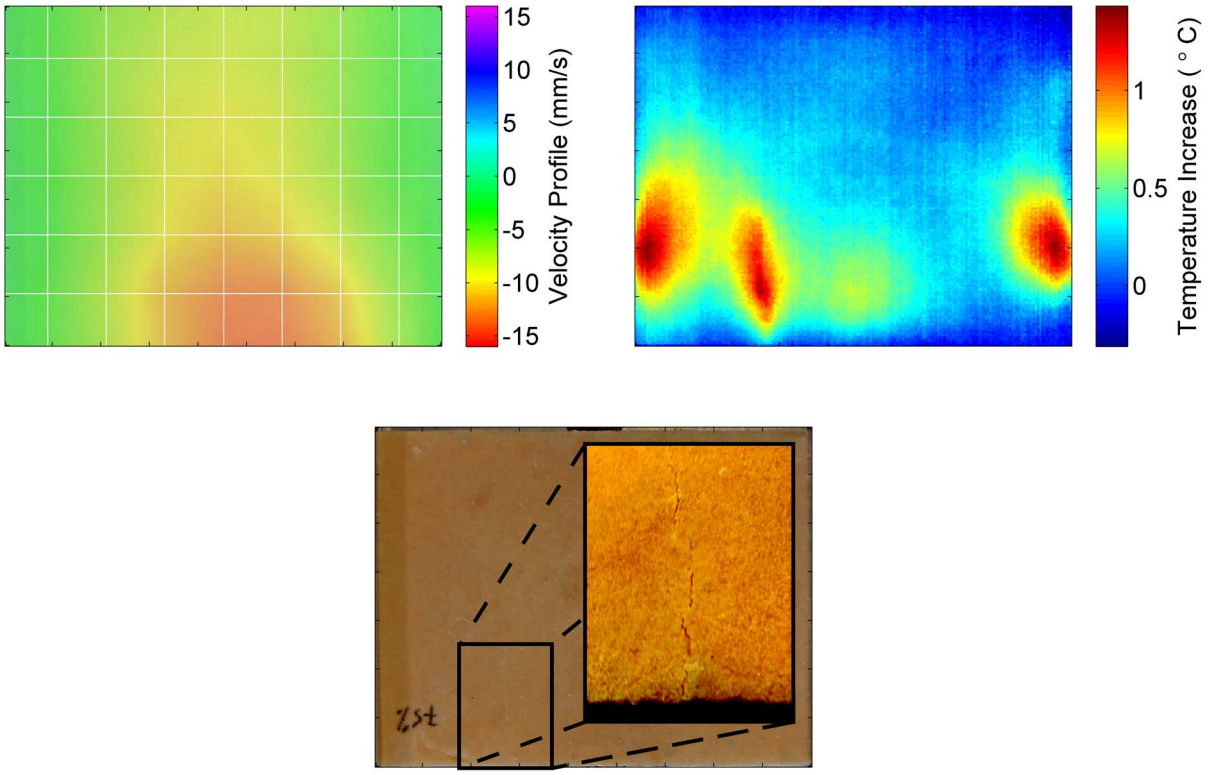


**FIGURE 12**: COMPARISON OF THE OBSERVED VELOCITY PROFILE AND THE STEADY-STATE SURFACE TEMPERATURE DISTRIBUTION OF THE 75% PLATE NEAR THE FIRST PORTION OF THE SPLIT FIRST RESONANCE. NOTE THAT THE OBSERVED ASYMMETRICAL TEMPERATURE INCREASE WAS IDENTIFIED AS THE SITE OF A CRACK IN THE SAMPLE FACE. THE CLOSE-UP PHOTO HAS BEEN COLOR-CORRECTED TO INCREASE CRACK VISIBILITY.

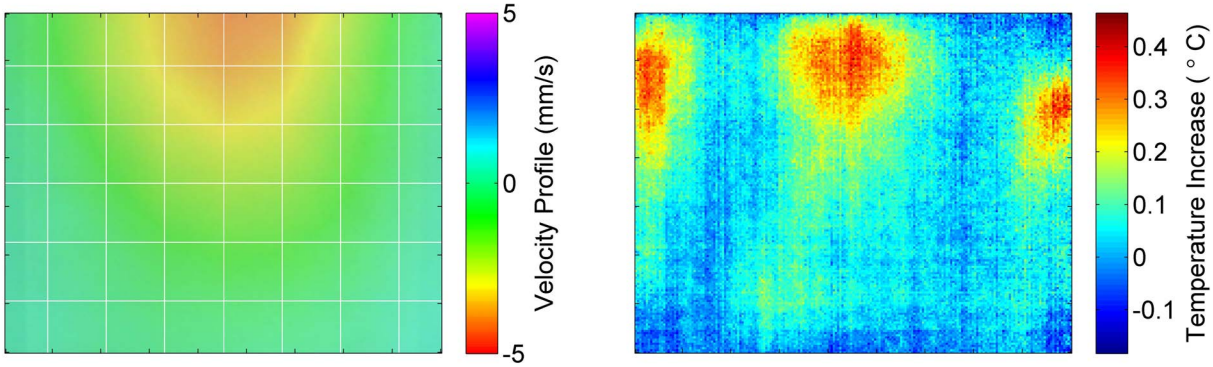


**FIGURE 13**: COMPARISON OF THE OBSERVED VELOCITY PROFILE AND THE STEADY-STATE SURFACE TEMPERATURE DISTRIBUTION OF THE 75% PLATE NEAR THE SECOND PORTION OF THE SPLIT FIRST RESONANCE. NOTE THAT THE EFFECT OF THE SURFACE DEFECT IS STILL VISIBLE, BUT DECREASED SIGNIFICANTLY IN MAGNITUDE.

## ACKNOWLEDGEMENTS

This research is supported by the U.S. Office of Naval Research under the Multidisciplinary University Research Initiative on Sound and Electromagnetic Interacting Waves through grant No. N00014-10-1-0958. The authors wish to acknowledge Chris Watson and Prof. Douglas Adams for their efforts related to sample preparation, and Jelena Paripovic and Prof. Patricia Davies for their efforts related to material property identification.

## REFERENCES

[1] Moore, D. S., 2007. "Recent Advances in Trace Explosives Detection Instrumentation". *Sensing and Imaging: An International Journal,* ***8***(1), pp. 9–38.

[2] Moore, D. S., 2004. "Instrumentation for Trace Detection of High Explosives". *Review of Scientific Instruments,* ***75***(8), pp. 2499–2512.

[3] Loginov, N. P., Muratov, S. M., and Nazarov, N. K., 1976. "Initiation of Explosion and Kinetics of Explosive Decomposition Under Vibration". *Combustion, Explosion, and Shock Waves,* ***12***(3), pp. 367–370.

[4] Loginov, N. P., 1997. "Structural and Physicochemical Changes in RDX Under Vibration". *Combustion, Explosion, and Shock Waves,* ***33***(5), pp. 598–604.

[5] Wakashima, K., and Tsukamoto, H., 1991. "Mean-field Micromechanics Model and its Application to the Analysis of Thermomechanical Behaviour of Composite Materials". *Materials Science and Engineering: A,* ***146***(1 - 2), pp. 291 – 316.

[6] Fu, S. Y., Feng, X. Q., Lauke, B., and Mai, Y. W., 2008. "Effects of Particle Size, Particle/Matrix Interface Adhesion and Particle Loading on Mechanical Properties of Particulate Polymer Composites". *Composites Part B: Engineering,* ***39***(6), pp. 933 – 961.

[7] Arefinia, R., and Shojaei, A., 2006. "On the Viscosity of Composite Suspensions of Aluminum and Ammonium Perchlorate Particles Dispersed in Hydroxyl Terminated Polybutadiene-New Empirical Model". *Journal of Colloid and Interface Science,* ***299***(2), pp. 962 – 971.

[8] Lewis, T. B., and Nielsen, L. E., 1970. "Dynamic Mechanical Properties of Particulate-Filled Composites". *Journal of Applied Polymer Science,* ***14***(6), pp. 1449–1471.

[9] Ratner, S. B., and Korobov, V. I., 1965. "Self-Heating of Plastics During Cyclic Deformation". *Polymer Mechanics,* ***1***(3), pp. 63–68.

[10] Renshaw, J., Chen, J. C., Holland, S. D., and Thompson, R. B., 2011. "The Sources of Heat Generation in Vibrothermography". *NDT & E International,* ***44***(8), pp. 736 – 739.

[11] Chervinko, O. P., 2004. "Calculating the Critical Parameters Characterizing the Thermal Instability of a Viscoelastic Prism with a Stress Concentrator Under Harmonic Compression". *International Applied Mechanics,* ***40***(8), pp. 916–922.

[12] Chervinko, O. P., Senchenkov, I. K., and Yakimenko, N. N., 2007. "Vibrations and Self-Heating of a Viscoelastic Prism with a Cylindrical Inclusion". *International Applied Mechanics,* ***43***(6), pp. 647–653.

[13] Luo, W., Yang, T., Li, Z., and Yuan, L., 2000. "Experimental Studies on the Temperature Fluctuations in Deformed Thermoplastics with Defects". *International Journal of Solids and Structures,* ***37***(6), pp. 887 – 897.

[14] Mignogna, R., Green Jr, R. E., Duke Jr, J. C., Henneke II, E. G., and Reifsnider, K. L., 1981. "Thermographic Investigation of High-power Ultrasonic Heating in Materials". *Ultrasonics,* ***19***(4), pp. 159–163.

[15] Zhang, W., 2010. "Frequency and Load Mode Dependence of Vibrothermography". Master's Thesis, Iowa State University.

[16] Katunin, A., and Fidali, M., 2012. "Self-Heating of Polymeric Laminated Composite Plates Under the Resonant Vibrations: Theoretical and Experimental Study". *Polymer Composites,* ***33***(1), pp. 138–146.

[17] Henneke II, E. G., Reifsnider, K. L., and Stinchcomb, W. W., 1986. "Vibrothermography: Investigation, Development, and Application of a New Nondestructive Evaluation Technique". Tech. Rep., DTIC Document.

[18] Paripovic, J., 2013. Personal Communication.